Published in final edited form as:
JACC Cardiovasc Imaging. 2010 April ; 3(4): 352–360. doi:10.1016/j.jcmg.2009.12.013.

Pericardial fat burden on ECG-gated noncontrast CT in asymptomatic patients who subsequently experience adverse cardiovascular events on 4-year follow-up: A case-control study

Victor Y. Cheng, MD[*,†], **Damini Dey, PhD**[*,†], **Balaji Tamarappoo, MD**[*], **Ryo Nakazato, MD**[*], **Heidi Gransar, MSc**[*], **Romalisa Miranda-Peats, MPH**[*], **Amit Ramesh, MSc**[*], **Nathan D. Wong, MD**[‡], **Leslee J. Shaw, PhD**[§], **Piotr J. Slomka, PhD**[*,†], and **Daniel S. Berman, MD**[*,†]

[*]Department of Imaging, Cedars-Sinai Medical Center, Los Angeles, California

[†]Department of Medicine, David Geffen School of Medicine, University of California, Los Angeles, California

[‡]Heart Disease Prevention Program, Department of Medicine, University of California, Irvine, California

[§]Department of Medicine, Division of Cardiology, Emory University School of Medicine, Atlanta, Georgia

Abstract

Background—Pericardial fat volume (PFV) and thoracic fat volume (TFV) can be routinely measured from noncontrast CT (NCT) performed for calculating coronary calcium score (CCS) and may predict major adverse cardiovascular event (MACE) risk.

Methods—From a registry of 2751 asymptomatic patients without known CAD and 4-year follow-up for MACE (cardiac death, myocardial infarction, stroke, late revascularization) after NCT, we compared 58 patients with MACE ("EVENTS") to 174 same-sex event-free controls matched by a propensity score to account for age, risk factors, and CCS. TFV was automatically calculated, and PFV was calculated with manual assistance in defining the pericardial contour, within which fat voxels were automatically identified. Independent relationships of PFV and TFV to MACE were evaluated using conditional multivariable logistic regression.

Results—EVENTS had higher mean PFV (101.8±49.2 cm^3 vs. 84.9±37.7 cm^3, p=0.007) and TFV (204.7±90.3 cm^3 vs. 177±80.3 cm^3, p=0.029) and higher frequencies of PFV>125 cm^3 (33% vs. 14%, p=0.002) and TFV>250 cm^3 (31% vs. 17%, p=0.025). After adjusting for Framingham Risk Score, CCS, and body-mass-index, PFV and TFV were significantly associated with MACE (odds ratio (OR) 1.74, 95%CI 1.03–2.95 for each doubling of PFV; OR 1.78, 95%CI 1.01–3.14 for TFV). Areas-under-the-curve from receiver operating characteristic analyses showed a trend of improved MACE prediction when PFV was added to FRS and CCS (0.73 vs 0.68, p=0.058). Addition of PFV, but not TFV, to FRS and CCS improved estimated specificity (0.72 vs 0.66, p=0.008) and overall accuracy (0.70 vs 0.65, p=0.009) in predicting MACE.

Corresponding Author: Daniel S. Berman, M.D., 8700 Beverly Blvd, Taper Building Room 1258, Los Angeles, CA 90048, Phone: 310-423-4223; daniel.berman@cshs.org.
Note: Dr. Cheng and Dr. Dey contributed equally to this work

Conflicts of Interest: None

Conclusion—Asymptomatic patients who experience MACE exhibit greater PFV on pre-MACE NCT when compared to event-free controls with similar cardiovascular risk profiles. Our preliminary findings suggest that PFV may help improve prediction of MACE.

Keywords

Pericardial fat; computed tomography; prognosis; cardiovascular events

INTRODUCTION

The discovery that pericardial fat may locally affect coronary arterial health through generation of inflammatory cytokines has generated a great level of interest in using it to predict adverse cardiovascular events (1). Pericardial fat can be routinely detected by noncontrast computed tomography (NCT) performed for coronary calcium scoring, potentially obviating the need for dedicated diagnostic testing. On NCT, pericardial fat volume (PFV) can be assessed by direct measurement, which depends on reliable detection of the thin pericardium, or as a component of heart-level intra-thoracic fat volume (TFV), whose boundaries are more robustly visualized, resulting in lower inter-observer variability (2,3).

To date, PFV detected on CT has been linked to coronary artery disease (CAD) risk factors, significant prior cardiovascular events, coronary arterial calcium, severity of detected CAD, and biochemical markers of systemic inflammation (2,4–12). However, whether PFV and TFV are related to occurrence of future adverse cardiovascular outcomes has not been evaluated. A case-control study design, often used to initially assess the epidemiologic importance of potentially novel disease markers and form the basis for subsequent prospective research (13–15), is advantageous for PFV and TFV, since complete quantification of both parameters in a large population using currently available techniques would be prohibitively time- and labor-intensive. We thus conducted the following case-control study to evaluate whether PFV and TFV predict subsequent major adverse cardiovascular events (MACE).

METHODS

Patient Population and Imaging protocol

Our study was a case-control analysis of 2751 asymptomatic patients without known CAD enrolled in the EISNER (Early Identification of Subclinical Atherosclerosis using Non-invasivE Imaging Research) registry at Cedars-Sinai Medical Center. Inclusion criteria for these patients were: adults 45–80 years in age who exhibited intermediate pre-test probability for CAD defined by being either 1) male ≥ 55 years-old or female ≥ 65 years-old or 2) male between 45–54 years-old or female between 55–64 years-old with at least 1 traditional CAD risk factor. Exclusion criteria were: History of myocardial infarction, coronary revascularization, cardiomyopathy, peripheral artery disease, angina, or stroke, history of having a prior coronary calcium scan or invasive coronary angiogram, active pregnancy, clinical instability, and significant medical co-morbidity likely to independently impact outcome during follow-up. Between September, 1998 and May, 2005, these patients underwent an index NCT to obtain a coronary calcium score (CCS) and was prospectively followed for subsequent MACE (including cardiac death, myocardial infarction, stroke, and late percutaneous or surgical revascularization defined as occurring more than 6 months after NCT). MACE was confirmed by direct contact between research staff and patient or next of kin, followed by review of corresponding medical or death records by an independent cardiologist.

At 4-years of follow-up, 58 patients (46 men) experienced MACE (EVENTS), including 4 cardiac deaths, 13 nonfatal myocardial infarctions, 8 strokes, 26 late percutaneous

revascularizations, and 7 late surgical revascularizations. We matched each EVENT to 3 same-sex event-free controls (CONTROLS) by using a propensity score; the technique of propensity score-based matching has been widely used to simultaneously control many confounders (16–18). An overall score was first calculated for each patient using a probit model that accounted for age, body mass index (BMI), traditional risk factors (diabetes, hypertension, dyslipidemia, smoking history, and family CAD history), and logarithm-adjusted CCS (since distribution of CCS was non-normal). Each EVENT was then matched to 3 same-sex CONTROLS with the closest scores. A total of 232 patients (58 EVENTS and 174 CONTROLS) thus comprised the study population. Framingham Risk Score (FRS) (19) was calculated for all patients at time of the index NCT. This study was conducted according to guidelines of the Cedars-Sinai Medical Center Institutional Review Board. All patients provided written consent for retrospective use of their data.

NCT was acquired using an electron-beam (e-Speed, GE Healthcare, Milwaukee, WI) or a 4-slice CT scanner (Somatom Volumezoom, Siemens Medical Solutions, Forchheim, Germany). Both scanners were calibrated daily using air and water phantoms. Each scan extended from the aortic arch to the diaphragm and was obtained during a single breath-hold. Scan parameters included: Heart-rate dependent ECG-triggering (typically 45–60% of the R-R interval), 35 cm field-of-view, and 512×512 matrix size. Tube voltage was 120 kVp with multislice scanning. Slice thickness was 3 mm for electron-beam CT and 2.5 mm for multislice CT.

All CT images were initially reviewed by an expert reader, using semi-automatic commercially available software (ScImage, Los Altos, CA) to quantify coronary calcification. Total Agatston CCS was calculated as the sum of calcified plaque scores of all coronary arteries (20). Acquired images were then transferred to a research workstation for pericardial and thoracic fat quantification.

Pericardial and Thoracic Fat Quantification

Definitions of pericardial and thoracic fat were based on our group's recent work (3): Pericardial fat includes all adipose tissue enclosed by the visceral pericardium, including all fat directly surrounding the coronary arteries. Thoracic fat includes all adipose tissue within the chest at the level of the heart, enclosed by the posterior limit of the heart and above the diaphragm, with the same cranial and caudal boundaries defined for pericardial fat. Thoracic fat includes pericardial fat.

Pericardial and thoracic fat quantification was performed by software (QFAT) developed at the Cedars-Sinai Medical Center (3). The software can be executed on standard MS Windows workstations and includes algorithms for automatic thoracic cavity and heart segmentation and quantification of thoracic fat, which we have already described (21). Image data was processed as follows. First, the upper slice limit, marked by bifurcation of the pulmonary trunk, and lower slice limit, identified as the last slice containing any portion of the heart, were manually chosen by an expert reader blinded to patient status and clinical NCT interpretation. Next, this reader defined 5–7 control points on the pericardium in each transverse view. From these control points, piecewise cubic Catmull-Rom spline functions (22) were automatically generated to create a smooth closed pericardial contour (see Figure 1). Pericardial and thoracic fat volumes were then automatically calculated. Contiguous 3D voxels between the Hounsfield Unit (HU) limits of −190 to −30 were defined as fat voxels by default (23–26); these limits could be modified by the user if deemed appropriate. PFV and TFV were reported in cm^3.

Statistical Analysis

Distributions of CCS, PFV, and TFV as continuous variables were non-normal and were thus described as mean ± standard deviation after normalization with logarithmic adjustment.

Base-2 logarithmic transformation was chosen since each unit increase represented a more easily understandable doubling of the variable in question; this approach has been adopted for CCS previously (27). Other continuous variables were described as mean ± standard deviation. Univariate comparisons between EVENTS and CONTROLS were made using the Student's t-test or the chi-squared test, as appropriate. Since individual covariate differences between EVENTS and CONTROLS after matching by propensity score can still cause confounding, conditional multivariable logistic regression models were constructed to adjust for these differences while assessing independent relationships between PFV, TFV, and MACE. This approach has been used previously (28,29). In the conditional multivariable regression models, PFV and TFV were entered into separate analyses containing age, CCS, and all traditional risk factors, and then into separate analyses containing BMI, CCS, and FRS. Model fit of the conditional logistic regression analyses were checked using the likelihood ratio test to evaluate whether addition of PFV and TFV yielded significant increases in deviance chi-square, which would suggest improved prediction of MACE. To further examine potential incremental value of PFV and TFV over established risk-prediction strategies, receiver-operating-characteristic (ROC) curves were constructed, and areas-under-the-curve (AUC) were compared. For all ROC analyses, FRS was a continuous variable; binary thresholds of 400 for CCS, 125 cm^3 for PFV, and 250 cm^3 for TFV were selected (PFV and TFV thresholds were found from initial comparisons between EVENTS and CONTROLS). Differences in estimated sensitivity, specificity, and accuracy were compared using the McNemar's test. Associations and differences with p-values < 0.05 were considered significant. All statistical analyses, including propensity score-based matching as described at the beginning of the Methods section, were performed using STATA software (Version 9, http://www.stata.com, StataCorp LP, Texas, USA).

RESULTS

Between EVENTS and matched CONTROLS, mean absolute differences in propensity score was 0.035±0.025. Our matching technique resulted in no significant differences in age, logarithm-adjusted CCS, and prevalence of traditional risk factors between EVENTS and CONTROLS (univariable analysis results are shown in Table 1). Hypercholesterolemia (66% in EVENTS, 64% in CONTROLS) and hypertension (81% in EVENTS, 80% in CONTRLS) were the most frequently found risk factors in both groups. Mean FRS in EVENTS was higher than that in CONTROLS at the time of NCT (15±8 vs. 12±7, p=0.012), though both mean scores predicted intermediate risk.

Detection of pericardial and thoracic fat and quantification of PFV and TFV was successful in all cases. Analysis of the typical NCT required 5–10 minutes of user time to fully contour the pericardium. PFV and TFV were highly correlated to each other (r^2=0.74).

Overall mean PFV was 89.1 ± 41.4 cm^3 (range 18.2–259.2 cm^3) and mean TFV was 183.9 ± 83.6 cm^3 (range 34.1–518.4 cm^3). EVENTS had greater mean PFV and TFV than CONTROLS (102±49 vs. 85±38 cm^3, p=0.007 and 205±90 vs. 177±80 cm^3, p=0.029, respectively). EVENTS had greater frequencies of PFV > 125 cm^3 (33% vs. 14%, p=0.002) and TFV > 250 cm^3 (31% vs. 17%, p=0.025). Figure 2 and Figure 3 each shows representative examples of pericardial and thoracic fat analysis in an EVENT and one of the corresponding controls.

Results from multivariable analyses are shown in Table 2 and Table 3. In multivariable analyses that adjusted for age, CCS, and all traditional risk factors, PFV was associated with MACE (OR 1.91, 95% CI 1.14–3.19 per doubling of PFV), as was TFV (OR 1.83, 95% CI 1.08–3.09 per doubling of TFV). As expected from matching, none of the other variables showed a significant association. In multivariable analyses that adjusted for BMI, CCS, and FRS, PFV (OR 1.74, 95% CI 1.03–2.95 per doubling) and TFV (OR 1.78, 95% CI 1.01–3.14 per doubling)

remained significantly associated with MACE. In these analyses, FRS was a concurrent independent predictor of MACE when adjusting for PFV (OR 1.10, 95% CI 1.03–1.17) or TFV (OR 1.10, 95% CI 1.03–1.17). Addition of PFV and TFV to the model containing BMI, CCS, and FRS significantly increased the deviance chi-square statistic (15.3 vs 10.8 for PFV, p=0.03; 14.9 vs 10.8 for TFV, p=0.04), indicating improved model fit. Extra-pericardial thoracic fat volume (TFV-PFV) did not exhibit a significant relationship to MACE when adjusting for BMI, CCS, and FRS (OR 1.44, 95% CI 0.91–2.28, p=0.12).

ROC analysis using FRS and CCS ≥ 400 resulted in an AUC of 0.68 and using FRS, CCS ≥ 400, and PFV ≥125 cm^3 resulted in an AUC of 0.73 (see Figure 4), a difference that trended towards significance (p = 0.058). Estimated sensitivity for predicting MACE when PFV ≥ 125 cm^3 was added to FRS and CCS ≥ 400 was not different than using FRS and CCS ≥ 400 only (0.65 vs 0.61, p=0.48). However, estimated specificity (0.72 vs 0.66, p = 0.009) and accuracy (0.70 vs 0.65, p =0.009) improved. ROC analysis using TFV ≥ 250 cm^3 in place of PFV did not show any significant difference (AUC 0.68 vs 0.68, p=0.7).

DISCUSSION

Our work is the first to directly evaluate the relationship between PFV, TFV and subsequent adverse cardiovascular outcomes. In our case-control study, based on 4-year post-NCT follow-up in asymptomatic patients without established CAD, we found that increased PFV was independently related to MACE. Although TFV (which includes PFV) also exhibited an independent relationship to MACE, a more detailed, ROC-based evaluation showed that PFV was the primarily responsible parameter. Furthermore, we found no significant relationship between extra-pericardial thoracic fat (defined as TFV-PFV) and MACE. Therefore, the association detected between TFV to MACE was in all likelihood due to TFV's close correlation to PFV.

Our findings provide an important insight into existing evidence linking PFV to markers of cardiovascular risk. In particular, we demonstrated that the potentially confounding associations between PFV, CAD risk factors, and CCS do not sufficiently explain the relationship between PFV and MACE (2,5,6,8–10,12). By using a propensity score to account for the totality of these confounders and generate adequately matched cohorts, we showed that PFV provided incremental value for predicting MACE. However, despite matching EVENTS to CONTROLS with many features used to derive FRS, our models did not fully control for FRS, which remained predictive of MACE. This finding highlights the strong prognostic utility of FRS in our population. Importantly, PFV still exhibited a significant association with MACE after adjustments for FRS.

Independent prognostic value of PFV for MACE may be a clinically relevant extension of previously described findings of elevated inflammation in pericardial fat depots. Mazurek, et al. elegantly showed that adipose tissue adjacent to the right coronary artery contained significantly higher expression of interleukin-1β, interleukin-6, monocyte chemotactic protein, and tumor necrosis factor, and retained a greater number of inflammatory cells than subcutaneous adipose tissue (1). A paracrine effect of inflammatory cytokines from pericardial adipose tissue may promote atherogenesis and lead to elevated risk of adverse coronary events, which made up the majority of MACE in our population (46 of 58 events, if death and stroke are counted as non-coronary events).

By definition, PFV and TFV are dependent variables. PFV has the advantage of being a more physiologically direct disease marker; however, it has the disadvantage of dependency on clear demarcation of the thin pericardium for quantification, making it more challenging, time-consuming, and potentially less reproducible to measure than TFV (3). An example of this was

seen in the work by Ding, et al., who measured TFV in a slab about the origin of the left main coronary in part because pericardium can be difficult to visualize in lean individuals (9). Mahabadi, et al. showed that PFV, but not intra-thoracic fat (equivalent to the extra-pericardial thoracic fat volume in our study), was related to burden of prior cardiovascular disease after adjusting for age, sex, BMI, and waist circumference, suggesting that PFV may be a more specific disease marker (11). However, Mahabadi, et al. did not examine the association between TFV and cardiovascular disease burden. There is also evidence suggesting that PFV and TFV may reflect risk of atherosclerotic disease in different regions within the body. Rosito, et al. showed that while PFV was associated with coronary calcification, TFV was associated with abdominal aortic calcification (10). Our work is the first to demonstrate that PFV is preferred over TFV when evaluating risk of clinically important cardiovascular outcomes.

We used an automated algorithm to quantify TFV (3,21) and a semi-automated approach, over a user-selected range of the heart, to quantify PFV. Logistically, automatic quantification of TFV is significantly less time-consuming (typically 20 seconds) and more reproducible (3). However, results from our present study suggest that fully automated algorithms for measurement of PFV can add to cardiovascular risk stratification and are needed for studying large patient cohorts.

Limitations

Our study had several limitations. The population evaluated comprised primarily of individuals at low-risk, and this was reflected in the modest number of adverse cardiovascular events. A case-control study design is more prone to confounding than a cohort study design; however, application of our semi-quantitative technique to measure whole-heart PFV in the entire cohort would have been prohibitively time and resource intensive, as noted. We used propensity score-based matching because simultaneous exact matching of all variables was not possible; propensity score-based matching may not be as powerful as individual variable matching in controlling for potential confounding. However, this design has been previously used with success (28,29). While our results suggest additive utility of pericardial fat to traditional MACE risk-stratifying tools, confirmation through longitudinal whole-cohort evaluation is needed. In addition, since individual risk factors were matched, we did not match for FRS to avoid redundancy.

CONCLUSION

Asymptomatic patients who experience MACE exhibited greater PFV on pre-MACE non-contrast CT than matched event-free controls with similar cardiovascular risk profiles. Our preliminary findings suggest that increased pericardial fat may help predict adverse cardiovascular outcomes.

Acknowledgments

This study was supported by NIH grant number R21EB006829-01A2 from the National Institute of Biomedical Imaging And Bioengineering (Dr. Dey) and the Glazer and Lincy Foundations in Los Angeles, California. We are also indebted to Dr. Arik Wolak for insights into pericardial fat quantification and Dr. Yuan Xu for assistance with statistical analysis.

Funding: NIH grant number R21EB006829 (Dr. Dey), the Glazer Foundation (Los Angeles, CA), and the Lincy Foundation (Los Angeles, CA)

ABBREVIATIONS

CAD	Coronary artery disease

CCS	Coronary calcium score
FRS	Framingham risk score
MACE	Major adverse cardiovascular event
NCT	Noncontrast computed tomography
PFV	Pericardial fat volume
TFV	Intra-thoracic fat volume

REFERENCES

1. Mazurek T, Zhang L, Zalewski A, et al. Human epicardial adipose tissue is a source of inflammatory mediators. Circulation 2003;108:2460–2466. [PubMed: 14581396]
2. Greif M, Becker A, von Ziegler F, et al. Pericardial adipose tissue determined by dual source CT is a risk factor for coronary atherosclerosis. Arterioscler Thromb Vasc Biol 2009;29:781–786. [PubMed: 19229071]
3. Dey D, Wong ND, Tamarappoo BK, et al. Computer-aided Non-contrast CT-based Quantification of Pericardial and Thoracic Fat and Their Associations with Coronary Calcium and Metabolic Syndrome. Atherosclerosis. 2009 Aug 21; Epub ahead of print.
4. Taguchi R, Takasu J, Itani Y, et al. Pericardial fat accumulation in men as a risk factor for coronary artery disease. Atherosclerosis 2001;157:203–209. [PubMed: 11427222]
5. Wheeler GL, Shi R, Beck SR, et al. Pericardial and visceral adipose tissues measured volumetrically with computed tomography are highly associated in type 2 diabetic families. Invest Radiol 2005;40:97–101. [PubMed: 15654254]
6. Fox CS, Massaro JM, Hoffmann U, et al. Abdominal visceral and subcutaneous adipose tissue compartments: association with metabolic risk factors in the Framingham Heart Study. Circulation 2007;116:39–48. [PubMed: 17576866]
7. Pou KM, Massaro JM, Hoffmann U, et al. Visceral and subcutaneous adipose tissue volumes are cross-sectionally related to markers of inflammation and oxidative stress: the Framingham Heart Study. Circulation 2007;116:1234–1241. [PubMed: 17709633]
8. Ding J, Kritchevsky SB, Harris TB, et al. The association of pericardial fat with calcified coronary plaque. Obesity (Silver Spring) 2008;16:1914–1919. [PubMed: 18535554]
9. Ding J, Kritchevsky SB, Hsu FC, et al. Association between non-subcutaneous adiposity and calcified coronary plaque: a substudy of the Multi-Ethnic Study of Atherosclerosis. Am J Clin Nutr 2008;88:645–650. [PubMed: 18779279]
10. Rosito GA, Massaro JM, Hoffmann U, et al. Pericardial fat, visceral abdominal fat, cardiovascular disease risk factors, and vascular calcification in a community-based sample: the Framingham Heart Study. Circulation 2008;117:605–613. [PubMed: 18212276]
11. Mahabadi AA, Massaro JM, Rosito GA, et al. Association of pericardial fat, intrathoracic fat, and visceral abdominal fat with cardiovascular disease burden: the Framingham Heart Study. Eur Heart J 2009;30:850–856. [PubMed: 19136488]
12. Sarin S, Wenger C, Marwaha A, et al. Clinical significance of epicardial fat measured using cardiac multislice computed tomography. Am J Cardiol 2008;102:767–7671. [PubMed: 18774004]
13. Birjmohun RS, Dallinga-Thie GM, Kuivenhoven JA, et al. Apolipoprotein A-II is inversely associated with risk of future coronary artery disease. Circulation 2007;116:2029–2035. [PubMed: 17923573]
14. Albert CM, Nam EG, Rimm EB, et al. Cardiac sodium channel gene variants and sudden cardiac death in women. Circulation 2008;117:16–23. [PubMed: 18071069]
15. Karthikeyan G, Teo KK, Islam S, et al. Lipid profile, plasma apolipoproteins, and risk of a first myocardial infarction among Asians: an analysis from the INTERHEART Study. J Am Coll Cardiol 2009;53:244–253. [PubMed: 19147041]
16. D'Agostino RB Jr. Propensity score methods for bias reduction in the comparison of a treatment to a non-randomized control group. Stat Med 1998;17:2265–2281. [PubMed: 9802183]

17. Stukel TA, Fisher ES, Wennberg DE, Alter DA, Gottlieb DJ, Vermeulen MJ. Analysis of observational studies in the presence of treatment selection bias: effects of invasive cardiac management on AMI survival using propensity score and instrumental variable methods. Jama 2007;297:278–285. [PubMed: 17227979]

18. D'Agostino RB Jr. Propensity Scores in Cardiovascular Research. Circulation 2007;115:2340–2343. [PubMed: 17470708]

19. Wilson PW, D'Agostino RB, Levy D, Belanger AM, Silbershatz H, Kannel WB. Prediction of coronary heart disease using risk factor categories. Circulation 1998;97:1837–1847. [PubMed: 9603539]

20. Agatston AS, Janowitz WR, Hildner FJ, Zusmer NR, Viamonte M Jr, Detrano R. Quantification of coronary artery calcium using ultrafast computed tomography. J Am Coll Cardiol 1990;15:827–832. [PubMed: 2407762]

21. Dey D, Suzuki Y, Suzuki S, et al. Automated quantitation of pericardiac fat from noncontrast CT. Invest Radiol 2008;43:145–153. [PubMed: 18197067]

22. Catmull, E.; Rom, R. A class of local interpolating splines; Proc. Of International Conference on Computer Aided Geometric Design; 1974. p. 317-326.

23. Yoshizumi T, Nakamura T, Yamane M, et al. Abdominal fat: standardized technique for measurement at CT. Radiology 1999;211:283–286. [PubMed: 10189485]

24. Kvist H, Chowdhury B, Grangard U, Tylen U, Sjostrom L. Total and visceral adipose-tissue volumes derived from measurements with computed tomography in adult men and women: predictive equations. Am J Clin Nutr 1988;48:1351–1361. [PubMed: 3202084]

25. Sjostrom L, Kvist H, Cederblad A, Tylen U. Determination of total adipose tissue and body fat in women by computed tomography, 40K, and tritium. Am J Physiol 1986;250:E736–E745. [PubMed: 3717334]

26. Wheeler GL, Shi R, Beck SR, et al. Pericardial and visceral adipose tissues measured volumetrically with computed tomography are highly associated in type 2 diabetic families. Invest Radiol 2005;40:97–101. [PubMed: 15654254]

27. Detrano R, Guerci AD, Carr JJ, et al. Coronary calcium as a predictor of coronary events in four racial or ethnic groups. N Eng J Med 2008;358:1336–1345.

28. Lindenauer PK, Pekow P, Wang K, et al. Lipid-lowering therapy and in-hospital mortality following major noncardiac surgery. JAMA 2004;291:2092–2099. [PubMed: 15126437]

29. Frolkis JP, Pothier CE, Blackstone EH, et al. Frequent ventricular ectopy after exercise as a predictor of death. N Eng J Med 2003;348:781–790.

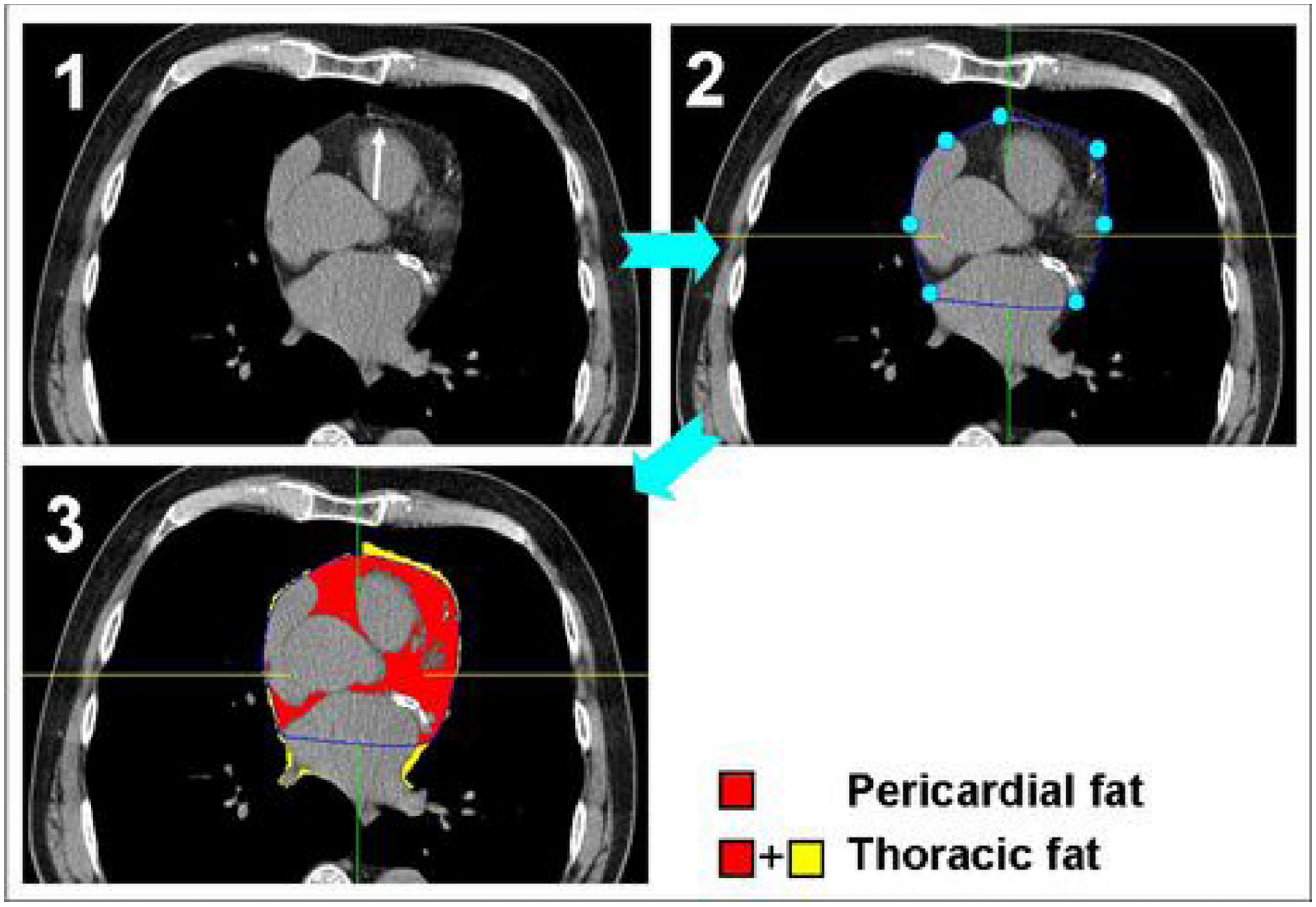

Figure 1.
Steps in semi-automatic pericardial fat volume (PFV) and thoracic fat volume (TFV) quantification. At each axial slice, the reader first identifies the pericardium (Panel 1, white arrow). Five-to-seven points are manually placed along the pericardial line, and a pericardial contour is then automatically generated (Panel 2). Once this task is completed for all axial slices, the software algorithm detects and quantifies all fat voxels within the pericardial contour to generate PFV. Fat voxels outside of the pericardial contour are also detected and added to PFV to generate TFV (Panel 3).

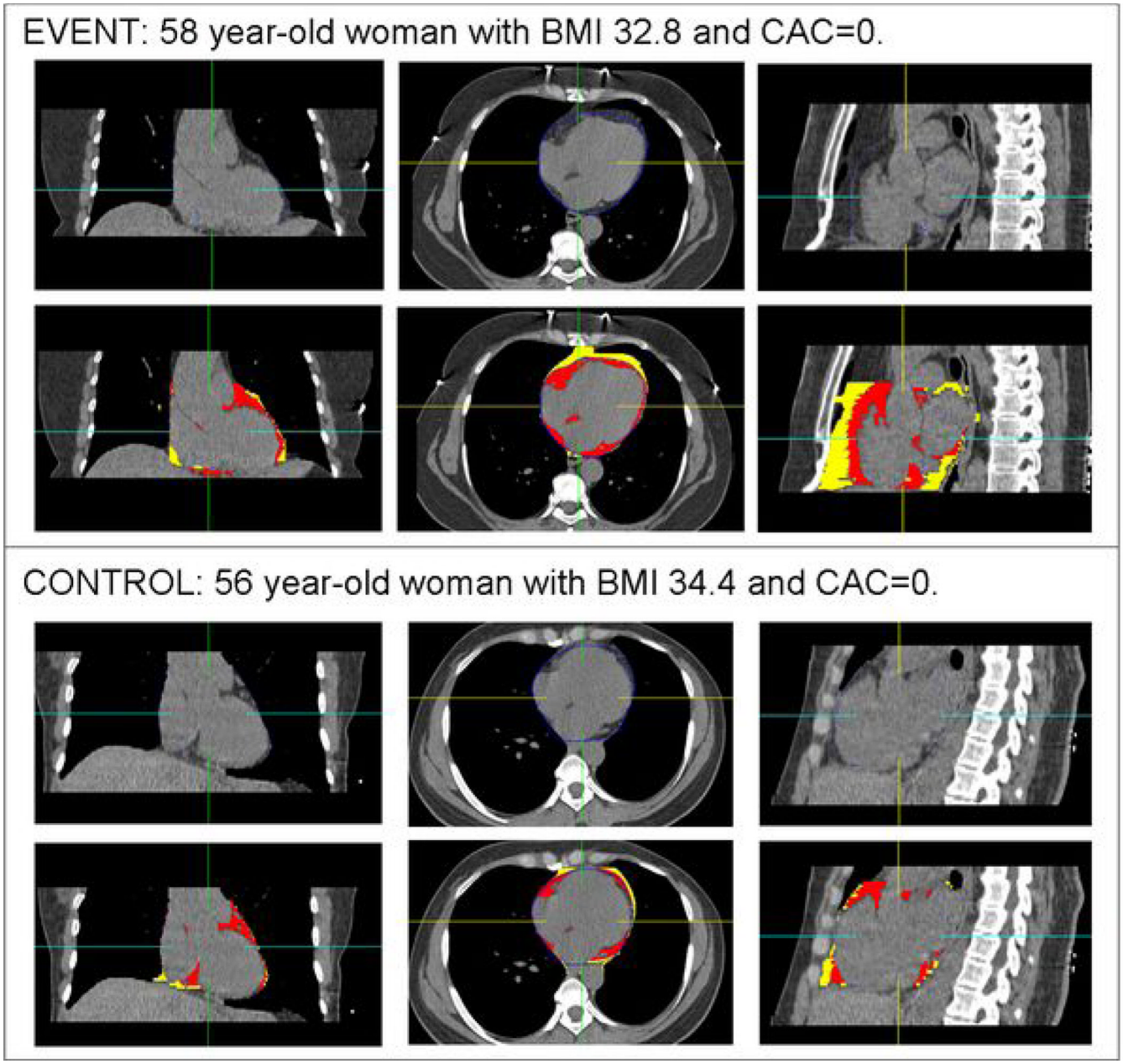

Figure 2.

A representative example of pericardial fat volume (PFV) and thoracic fat volume (TFV) quantification in matched patients with a coronary calcium score (CCS) of 0. Within each panel, the top row shows standard coronal, axial, and sagittal (left to right) CT displays of the heart, and the bottom row shows the same images with superimposed detection of pericardial fat (red) and thoracic fat (red and yellow). Top panel images are from a 58 year-old woman who underwent coronary artery bypass graft surgery for symptomatic multi-vessel coronary artery disease 572 days after the noncontrast CT. Her PFV was 187 cm^3 and TFV was 315 cm^3. Bottom panel images are from a matched 56 year-old event-free woman. Her PFV was 72 cm^3 and TFV was 111 cm^3.

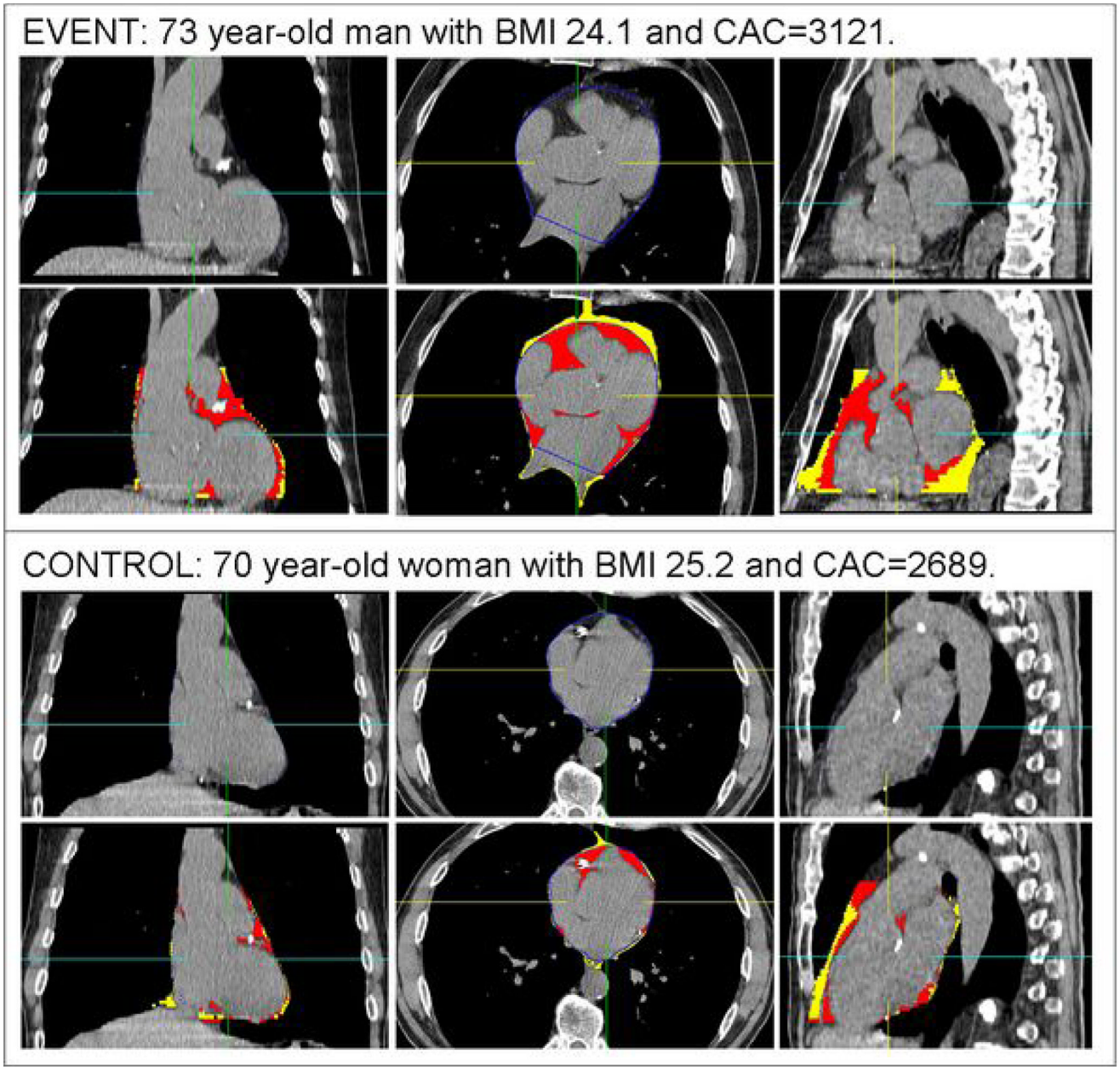

Figure 3.

A representative example of pericardial fat volume (PFV) and thoracic fat volume (TFV) quantification in matched patients with very high coronary calcium scores (CCS). Within each panel, the top row shows standard coronal, axial, and sagittal (left to right) CT displays of the heart, and the bottom row shows the same images with superimposed detection of pericardial fat (red) and thoracic fat (red and yellow). Top panel images are from a 73 year-old man with a CCS of 3121 who suffered a nonfatal myocardial infarction 99 days after the noncontrast CT. His PFV was 170 cm^3 and TFV was 329 cm^3. Bottom panel images are from a matched 70 year-old event-free man with a CCS of 2689. His PFV was 78 cm^3 and TFV was 137 cm^3.

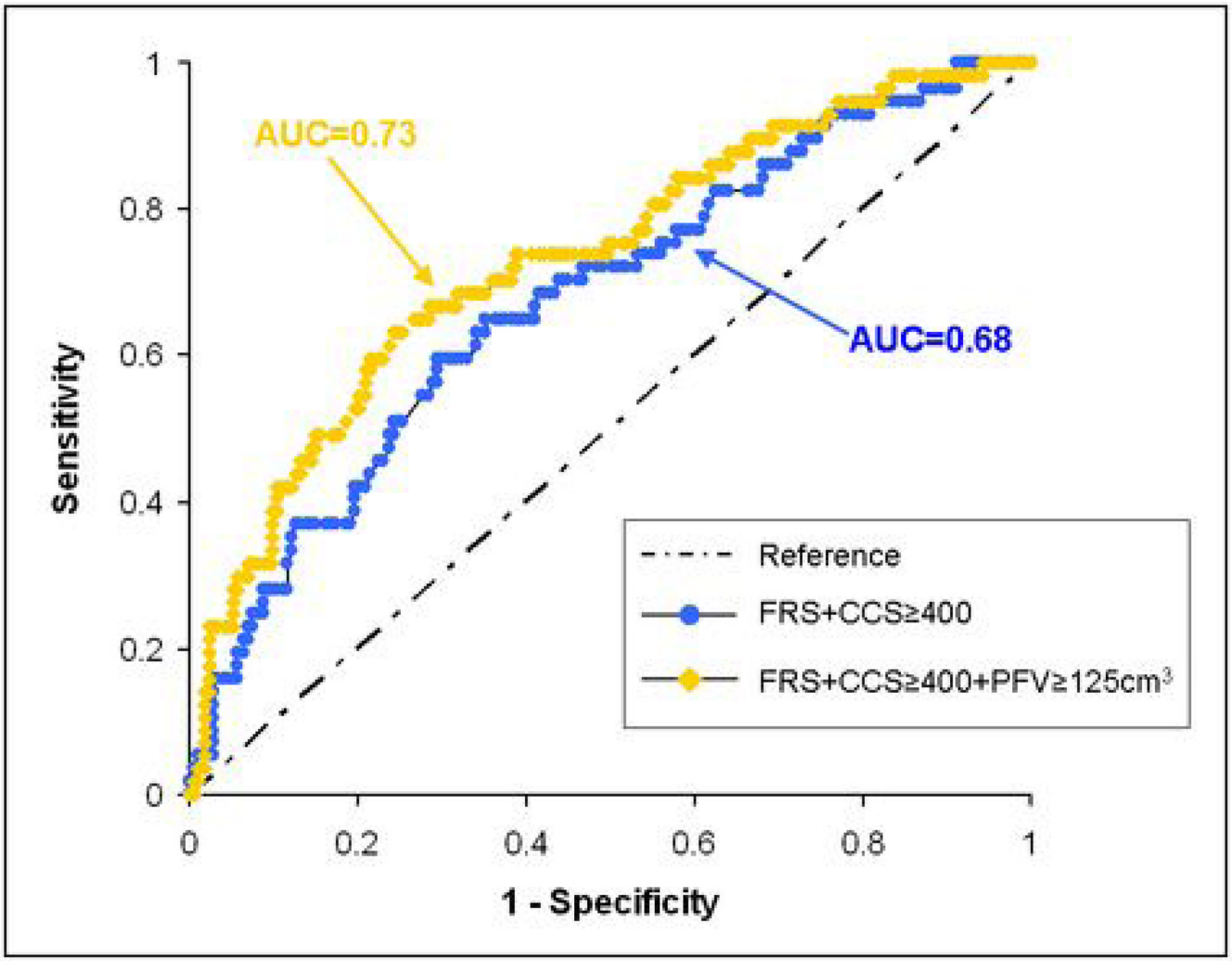

Figure 4.
Receiver-operator-characteristic curves for major adverse cardiovascular event (MACE) prediction using Framingham Risk Score (FRS) and coronary calcium score greater than 400 (CCS≥400) only and using FRS, CCS≥400, and pericardial fat volume greater than 125 cm^3 ($PFV \geq 125 cm^3$). Areas-under-the-curve for FRS+CCS≥400+PFV≥125cm3 indicated a trend towards improved prediction compared to FRS+CCS≥400 only (0.73 vs 0.68, p = 0.058).

Table 1

Characteristics of 58 patients with MACE (EVENTS) and 174 matched event-free controls (CONTROLS). Matched variables are shown in *italics*.

	EVENTS (mean±SD or %)	**CONTROLS (mean±SD or %)**	**p value**
Age	*61 ± 10*	*61 ± 8*	*0.70*
Male sex	*79 %*	*79 %*	*1.00*
BMI	*28.8 ± 5.7*	*28.3 ± 4.7*	*0.57*
Diabetes	*19 %*	*17 %*	*0.69*
Hypertension	*66 %*	*64 %*	*0.87*
Hypercholesterolemia	*81 %*	*80 %*	*0.92*
Active smoking	*12 %*	*9 %*	*0.44*
Family CAD history	*24 %*	*21 %*	*0.65*
*$Log_2(CCS)$**	*7.2 ± 3.1*	*7.0 ± 2.7*	*0.65*
Framingham Risk Score	15 ± 8	12 ± 7	0.01

BMI=body mass index, CAD=coronary artery disease, CCS=coronary calcium score, MACE=major adverse cardiovascular event, SD= standard deviation

* Logarithmic transform of CCS was performed to adjust for its non-normal distribution

Table 2

Results of conditional multivariable regression analyses adjusting for age, traditional risk factors, and CCS

	Odds Ratio (95% CI)	p value
Analysis with PFV		
Age	1.00 (0.96–1.06)	0.72
Diabetes	1.49 (0.60–3.70)	0.39
Hypertension	1.01 (0.50–2.07)	0.97
Hypercholesterolemia	1.15 (0.51–2.57)	0.74
Active smoking	2.57 (0.76–8.70)	0.13
Family CAD history	1.28 (0.54–3.05)	0.57
$Log_2(CCS)^*$	1.07 (0.90–1.28)	0.43
$Log_2(PFV)^*$	1.91 (1.14–3.19)	0.01
Analysis with TFV		
Age	1.01 (0.96–1.07)	0.60
Diabetes	1.38 (0.56–3.41)	0.48
Hypertension	0.96 (0.47–1.97)	0.92
Hypercholesterolemia	1.11 (0.50–2.47)	0.80
Active smoking	2.56 (0.76–8.65)	0.13
Family CAD history	1.26 (0.53–2.99)	0.60
$Log_2(CCS)^*$	1.06 (0.89–1.26)	0.53
$Log_2(TFV)^*$	1.83 (1.08–3.09)	0.02

CAD=coronary artery disease, CCS=coronary calcium score, CI=confidence interval, PFV=pericardial fat volume, TFV=intra-thoracic fat volume

*Logarithmic transform of CCS, PFV, and TFV were performed to adjust for their non-normal distributions

Table 3

Results of conditional multivariable regression analyses adjusting for BMI, CCS, and FRS

	Odds Ratio (95% CI)	p value
Analysis with PFV		
BMI	0.98 (0.92–1.06)	0.661
$Log_2(CCS)^*$	1.06 (0.90–1.25)	0.473
FRS	1.10 (1.03–1.17)	0.003
$Log_2(PFV)^*$	1.74 (1.03–2.95)	0.038
Analysis with TFV		
BMI	0.97 (0.90–1.05)	0.484
$Log_2(CCS)^*$	1.05 (0.89–1.24)	0.548
FRS	1.10 (1.03–1.17)	0.003
$Log_2(TFV)^*$	1.78 (1.01–3.14)	0.047

CCS=coronary calcium score, CI=confidence interval, FRS=Framingham Risk Score, PFV=pericardial fat volume, TFV=intra-thoracic fat volume

* Logarithmic transform of CCS, PFV, and TFV were performed to adjust for their non-normal distributions